

Research Paper

DYNAMIC RESPONSE OF STRUCTURE WITH SEMI-ACTIVE TUNED MASS FRICTION DAMPER

Alka Y Pisal^{1*} and R S Jangid¹

*Corresponding Author: **Alka Y Pisal**, ✉ alka.pisal@iitb.ac.in

A passive tuned mass friction damper (P-TMFD) has a pre-determined and fixed slip force at which it can reduce the response of the structure effectively. At any value other than the pre-determined slip force, it loses its effectiveness and simply behaves as a normal bracing system. Also, P-TMFD changes its state between stick and slip mode many times during a seismic or harmonic excitation which results in high frequency response of the system and reduces its efficiency. To overcome the disadvantage of P-TMFD, a semi-active tuned mass friction damper (SA-TMFD) is proposed. The control algorithm proposed by Lu (2004) which is known as Predictive control law, is used. The SA-TMFD produces continuous and smooth slip force and eliminates the high frequency response of the structure which usually occurs in case of P-TMFD. The governing differential equations of motion of the SDOF system with SA-TMFD are solved numerically using state-space method. To investigate the effectiveness of SA-TMFD with predictive control, the responses of the structure with SA-TMFD are compared with the responses of the structures with P-TMFD under harmonic and earthquake excitations. The result of numerical studies indicated that the SA-TMFD is more effective and has better performance level than the P-TMFD for a same input seismic and harmonic excitations.

Keywords: P-TMFD, SA-TMFD, Predictive control, Numerical analysis, Harmonic response, Seismic control

INTRODUCTION

A Tuned Mass Damper (TMD) is a combination of an added mass with spring and damping element that reduces the response of the primary system to which it is attached by vibrating out of phase with the main system in resonance condition. Unlike TMD, the dry Friction Dampers (FD) dissipates energy through sliding, having friction between

adjoining surfaces. The literature review shows that some authors have explored the response of the system with P-TMFD. Ricciardelli and Vickery (1999) considered a SDOF system to which a TMD with linear stiffness and dry friction damping was attached. The system was analyzed for harmonic excitation and design criteria for friction TMD system were proposed. Zeng Gewei *et al.* (2010) used

¹ Department of Civil Engineering, Indian Institute of Technology Bombay, Powai, Mumbai 400076, India.

Harmonic and static linearization solutions to analyze dynamic characteristics of SDOF system with friction tuned mass damper. P-TMFD is having advantage that it can behave either as a FD when it is in slip-state and as an added mass when it is in stick state. On the other hand, the disadvantage of P-TMFD is that it has a pre-determined and a fixed value of slip force at which it reduces the response of the system to which it is attached, when it is in slip mode. At too small and too high value of slip force, the damper will not slip for the most of the harmonic and earthquake excitation duration and thus the capacity of P-TMFD to reduce structural response may not be fully utilized. Also during an earthquake P-TMFD vibrate in two different modes (i.e. stick state and slip state), many times which results in high-frequency structural responses which are undesirable.

In order to improve the performance of such passive devices, the concept of semi-active control was emerged. The advantage of semi-active control system is that it is able to adjust its slip force by controlling its clamping force in real time with respect to the response of the structure during an excitation. Dowdell and Cherry (1994) and Kannan *et al.* (1995) were among the first researchers to study the response of structures with semi-active friction dampers. They adopted on-off and bang-bang control methods for their study. Inaudi (1997) proposed modulated homogeneous friction control algorithm which produces a slip force proportional to the prior local peak of the damper deformation. Akbay and Aktan (1995) proposed a control algorithm that determines the clamping force in next time step by one pre-specified increment of the current force at

a fixed time step. Also, the literature review shows that the control performance of semi-active dampers fully depends on the applied control algorithm. There have been many studies on the development of the control law. Spencer *et al.* (1997) proposed phenomenological model for magnetorheological damper. Dowdell and Cherry (1996) proposed semi-active control law which is modified from optimal control. Lu and Lin (2002) presented the control law modified from the modal control. Most of the developed algorithm either produces the discontinuous control forces or partially continuous slip forces. In both the cases the damper capacity may not be fully used. Recently, Lin *et al.* (2010) proposed SAF-TMD and investigated the effectiveness of SAF-TMD in protecting structures subjected to seismic forces using non-sticking law.

It is also observed that the semi-active control algorithms are developed specifically for TMD and for FD, but limited algorithms are developed for P-TMFD. In this study the performance of a SA-TMFD attached to a damped SDOF system is investigated for harmonic and seismic ground excitations. The control algorithm developed by Lu (2004), known as predictive control is applied to SA-TMFD to get a continuous smooth slip force, so that it remains in its slip state during entire earthquake duration. The specific objectives of the study are summarized as: (i) To identify a appropriate parameter which controls the desired responses of the SDOF system with SA-TMFD, (ii) to investigate the effect and optimum value of gain multiplier for the response reduction of the controlled SDOF system; and (iii) to investigate the effectiveness of SA-TMFD in response reduction under the harmonic and earthquake excitations.

MODELING OF SDOF SYSTEM WITH SA-TMFD

The primary/main system equipped with SA-TMFD is shown in Figure 1 schematically. The SA-TMFD applies variable friction force on the primary system. The variable friction force of SA-TMFD can be controlled by varying the clamping force.

The schematic model of the Two Degree of Freedom (TDOF) system shows that in Figure 1, m_1 , k_1 and c_1 represents the mass, linear stiffness and viscous damping of main/primary system, respectively. The natural frequency, damping ratio and time period of the primary system are $\omega_1 = \sqrt{k_1/m_1}$, $\xi_1 = c_1/2\sqrt{k_1m_1}$ and $T_{n1} = 2\pi/\omega_1$, respectively. The SA-TMFD installed on primary system has mass m_2 , stiffness k_2 and self adjusting variable friction

force F_d . The natural frequency of secondary system is $\omega_2 = \sqrt{k_2/m_2}$. The mass ratio and tuning ratio of the two systems are defined as $\mu = m_2/m_1$ and $\Omega = \omega_2/\omega_1$, respectively; where μ represents the mass ratio and Ω represents the tuning ratio.

EQUATIONS OF MOTION FOR DYNAMIC EXCITATION

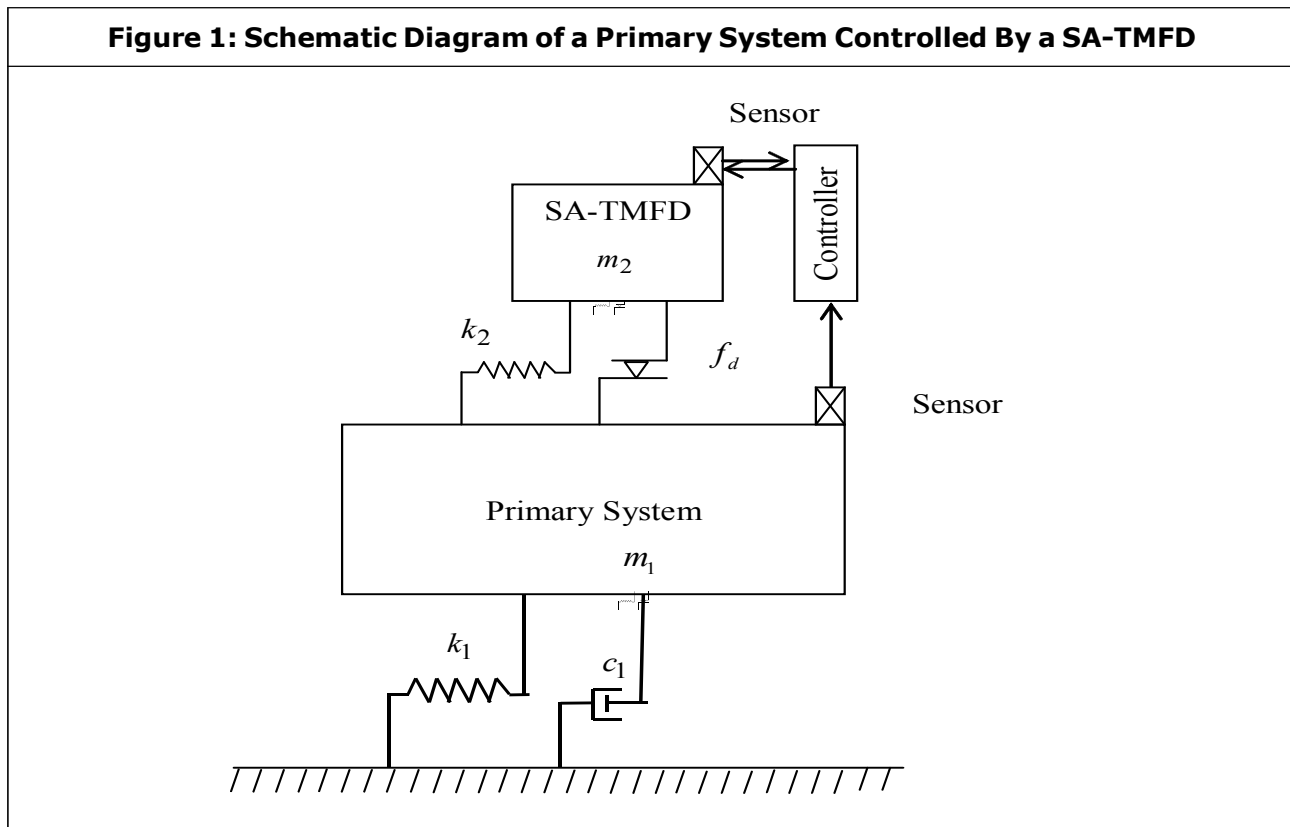
The governing equations of motion of TDOF system when subjected to dynamic excitations are expressed as

$$m_1\ddot{x}_1 + c_1\dot{x}_1 + k_1x_1 + k_2(x_1 - x_2) = -m_1\ddot{x}_g + F_d \operatorname{sgn}(\dot{x}_2 - \dot{x}_1) \quad \dots(1a)$$

$$m_2\ddot{x}_2 - k_2(x_1 - x_2) = -m_2\ddot{x}_g - F_d \operatorname{sgn}(\dot{x}_2 - \dot{x}_1) \quad \dots(1b)$$

Equation (1) can be written as

$$M \ddot{X}_{(t)} + C \dot{X}_{(t)} + K X_{(t)} = E \ddot{x}_{g(t)} + B F_{d(t)} \quad \dots(2)$$



where

$$X_{(t)} = \begin{Bmatrix} x_{1(t)} \\ x_{2(t)} \end{Bmatrix} \quad \text{and} \quad Z_{(t)} = \begin{Bmatrix} x_{1(t)} \\ x_{2(t)} \\ \dot{x}_{1(t)} \\ \dot{x}_{2(t)} \end{Bmatrix} \quad \dots(3)$$

and

$$M = \begin{bmatrix} m_1 & 0 \\ 0 & m_2 \end{bmatrix}, \quad C = \begin{bmatrix} c_1 & 0 \\ 0 & 0 \end{bmatrix}, \quad K = \begin{bmatrix} k_1 + k_2 & -k_2 \\ -k_2 & k_2 \end{bmatrix}$$

$$M = \begin{bmatrix} m_1 & 0 \\ 0 & m_2 \end{bmatrix}, \quad C = \begin{bmatrix} c_1 & 0 \\ 0 & 0 \end{bmatrix}, \quad K = \begin{bmatrix} k_1 + k_2 & -k_2 \\ -k_2 & k_2 \end{bmatrix}$$

$$E = \begin{bmatrix} 0 \\ -1 \end{bmatrix}, \quad B = \begin{bmatrix} 0 \\ M^{-1}L \end{bmatrix}, \quad L = [-1]$$

The matrix E and B are placement matrices for the excitation force and friction force, respectively. Also, $x_{1(t)}$ and $x_{2(t)}$ shows the relative displacement of the primary and secondary system with respect to ground, respectively.

SOLUTION OF EQUATIONS OF MOTION

Equation (2) can be formulated in dynamic state space as

$$\dot{Z}_{(t+1)} = AZ_{(t+1)} + E\ddot{x}_{g(t+1)} + BF_{d(t+1)} \quad \dots(4)$$

where, vector $Z_{(t)}$ denotes the state of the structure as shown in Equation (3), $F_{d(t)}$ denotes the vector of controllable friction force provided by the SA-TMFD, $\ddot{x}_{g(t)}$ is the ground acceleration, A represents the system matrix that is composed of structural mass, stiffness

and damping matrices. When the Equation (5) is further discretized in the time domain assuming excitation force to be constant within any time interval, Equation (5) can be converted into a discrete time form as mentioned by Meirovitch (1990).

$$Z_{(j+1)} = A_d Z_{(j)} + E_d \ddot{x}_{g(j)} + B_d F_{d(j)} \quad \dots(5)$$

where, subscripts (j) and (j+1) denotes that the variables are evaluated at the (j)th and (j+1)th time step.

$$B_d = A^{-1}(A_d - I)B \quad \dots(6a)$$

$$E_d = A^{-1}(A_d - I)E \quad \dots(6b)$$

Also, $A_d = e^{A\Delta t}$ denotes the discrete-time system matrix with Δt as the time interval.

Let y be a vector showing damper displacement which is equal to the storey drift i.e., $y = x_2 - x_1$. At any instant of time the relation between damper displacement y and state of the structure z may be written as

$$y_{(j)} = DZ_{(j)} \quad \dots(7)$$

where, D is a constant matrix of dimension (r × 2n); n is the number of DOFs of the structure, and r is the total number of SA-TMFDs. Furthermore, the damper displacement consists of two components.

$$y_{(j)} = y_{r(j)} + y_{b(j)} \quad \dots(8)$$

where, $y_{r(j)}$ represents the slip displacements on the friction interfaces of the damper, while $y_{b(j)}$ represents the elastic deformations of the dampers, which are proportional to the axial forces of the dampers. The axial forces of the FD are equivalent to the friction forces,

therefore, by the elastic constitutive law for axial members, we have

$$F_{d(j)} = k_2 \cdot y_{b(j)} \quad \dots(9)$$

where, k_2 is a ($r \times r$) diagonal matrix consists of stiffness of the SA-TMFD.

$$F_{d(j)} = k_2 [D Z_{(j)} - y_{r(j)}] \quad \dots(10)$$

As it is clear from Equation (10), the friction force vector $F_{d(j)}$ is a function of the current structural state $Z_{(j)}$ as well as the slip displacement on the friction interfaces of the two systems $y_{r(j)}$. At any given time instant the SA-TMFD can remains only in one state, i.e., either in stick state or in slip state. During the time interval from $(j - 1)^{th}$ to $(j)^{th}$ time step, if the damper is in stick state then it should satisfy the following condition.

$$y_{r(j)} = y_{r(j-1)} \quad \dots(11)$$

By applying the results of Equations (10) and (11), the subtraction of $F_{d(j-1)}$ and $F_{d(j)}$ leads to

$$F_{d(j)} = k_2 D [Z_{(j)} - Z_{(j-1)}] + F_{d(j-1)} \quad \dots(12)$$

Now, introducing Equation (5) into Equation (12) and replacing subscript (j) by $(j-1)$ leads to

$$\tilde{F}_{d(j)} = G_z Z_{(j-1)} + G_{xg} \ddot{x}_{g(j-1)} + G_{fd} F_{d(j-1)} \quad \dots(13)$$

where

$$\left. \begin{aligned} G_z &= k_2 D (A_d - I) \\ G_{xg} &= k_2 D E_d \\ G_{fd} &= k_2 D B_d + I \end{aligned} \right\} \quad \dots(14)$$

Note that in Equation (13), $\tilde{F}_{d(j)}$ shows the damper force computed by assuming that the

damper is in stick state which may not be equal to actual friction force $F_{d(j)}$. As vector $\tilde{F}_{d(j)}$ plays a very important role in deciding the state (either stick or slip) and actual friction force in the damper. It shows the minimum friction force required by the damper at the t^{th} time step to remain in stick state and thus it is referred as 'critical friction force'. Equation (13) shows that vector $\tilde{F}_{d(j)}$ can be computed easily, once $Z_{(j-1)}$, $F_{d(j-1)}$ and $\ddot{x}_{g(j-1)}$ have been determined at the previous time step. Further, it is assumed that damper obeys Coulomb's friction law. In this case the actual friction force vector $F_{d(j)}$ and critical friction force vector $\tilde{F}_{d(j)}$ shall be reduce to scalars $F_{d(j)}$ and $\tilde{F}_{d(j)}$. The state of the damper can be decided to be

Stick state, if

$$|\tilde{F}_{d(j)}| < F_{d \max(j)} = F_c N_{(j)} \quad \dots(15a)$$

Slip state, if

$$|\tilde{F}_{d(j)}| \geq F_{d \max(j)} = F_c N_{(j)} \quad \dots(15b)$$

where, F_c is the friction coefficient and $N_{(j)}$ is the time varying clamping force of the damper. Using these equations, once the state of the damper is determined, its frictional force can be calculated by

$$F_{d(j)} = \tilde{f}_{d(j)} \quad (\text{for stick state})$$

$$F_{d(j)} = \text{sgn}[\tilde{f}_{d(j)}] F_c N_{(j)} \quad (\text{for slip state}) \quad \dots(16)$$

where, sgn denotes the signum function which takes the sign of variable and is used to denote the direction of the resisting slip force. Once $F_{d(j)}$ is obtained from Equation (16) and substituted into Equation (5), the structural response $Z_{(j+1)}$ can be determined and then the response of the system in next time step can be simulated.

Equation (15b) shows that if the clamping force $N_{(j)}$ is applied in such a way that resulting slip force is always slightly less than the value $\tilde{F}_{d(j)}$ predicted by Equation (13) then the damper will remain in the slip state for the complete duration of the harmonic or earthquake excitation. Based on this concept, the control rule for determining the clamping force of a semi-active friction damper is proposed by Lu (2004) as

$$N_{(j)} = \alpha \frac{|\tilde{F}_{d(j)}|}{F_c}, \quad 0 \leq \alpha \leq 1 \quad \dots(17)$$

where, α is a selectable constant parameter known as gain multiplier and $\tilde{F}_{d(j)}$ is obtained from Equation (13), substituting $N_{(j)}$ from Equation (17) into Equation (15b), keeps the Equation (15b) always true for the damper and keep the damper in its slip state. Therefore the damper friction forces can be computed by substituting Equation (17) into Equation (15) and re-writing it in a vector form as

$$\mathbf{F}_{d(j)} = \alpha \tilde{\mathbf{F}}_{d(j)} \quad \dots(18)$$

Equation (18) shows that if the value of α is such as $0 \leq \alpha \leq 1$, damper friction force vector $\mathbf{F}_{d(j)}$ will be always less than $\tilde{\mathbf{F}}_{d(j)}$. By using Equation (13) in Equation (18), one can obtains an explicit formula to calculate the control force vector as

$$\mathbf{F}_{d(j)} = \alpha \left\{ \begin{matrix} G_z \cdot Z_{(j-1)} + G_{fd} \cdot \mathbf{F}_{d(j-1)} \\ + G_{xg} \cdot \ddot{x}_{g(j-1)} \end{matrix} \right\} \quad \dots(19)$$

From Equation (19), it is noted that the parameter α plays an important role in the proposed predictive control law.

NUMERICAL STUDY

For the numerical study the damping ratio and natural frequency of the SDOF system are taken as 2% and 2 Hz, respectively. The mass ratio, μ , is taken as 2% of the weight of the SDOF system and the frequency ratio, Ω , is taken as 0.98.

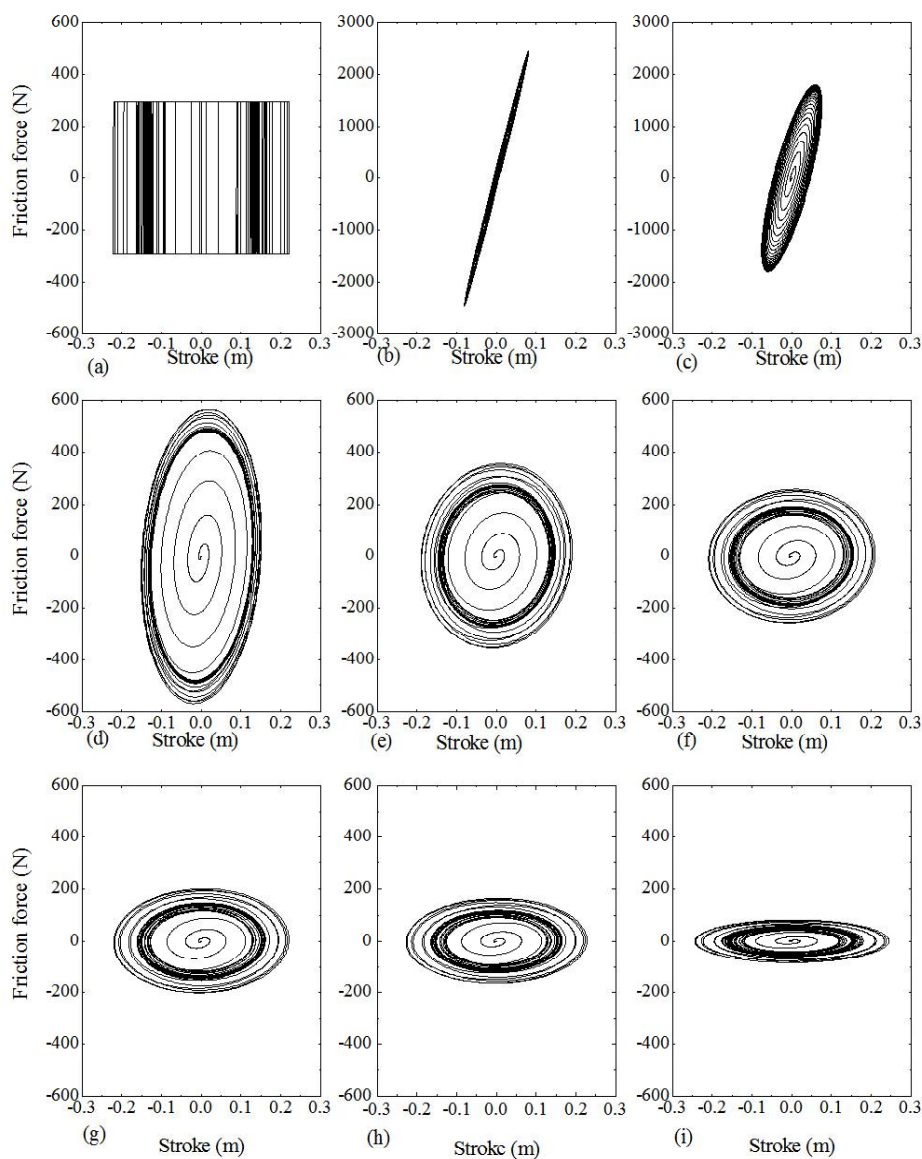
Numerical Study for Harmonic Excitation

In this section, the response of primary system with SA-TMFD subjected to harmonic ground acceleration is investigated. The harmonic excitation is taken as $\ddot{x}_{g(t)} = 0.05g \sin(4\pi t)$. The important parameter α on which the efficiency of SA-TMFD depends is investigated. The effectiveness of the SA-TMFD is investigated by comparing the response of the system with corresponding P-TMFD. For the present study, the results are obtained with time interval, $\Delta t = 0.02$. The number of iteration in each time step is taken as 200 to determine the incremental frictional force in the P-TMFD and SA-TMFD. It is to be noted that the energy dissipation capacity of a device is usually understood by its hysteresis loop. In case of semi-active device, its hysteresis loop depends mainly on the applied control algorithm. It means, the same semi-active device have different hysteretic behaviors under different control algorithms. For the study and comparison purpose, the hysteresis loop of P-TMFD having pre-fixed slip force equal to 15% of the weight of the P-TMFD is plotted in Figure 2(a). For P-TMFD, hysteretic continuous model proposed by Constantinou *et al.* (1990) using Wen's equation (Wen, 1976) is used. The non-dimensional parameters which control the shape of the loop are selected in such a way

that it provides typical Coulomb-friction damping. The recommended values of these parameters are taken as $q = 0.0001$ m, $A = 1$, $\beta = 0.5$, $\tau = 0.05$, $n = 2$, (Bhaskararao and Jangid, 2006), where q represents the yield

displacement of frictional force loop and A, β, τ and n are constants. Also, the hysteresis loops of SA-TMFD are plotted with different values of α in Figure 2(b) to 2(i). In this figure, the slip friction force developed in the damper is

Figure 2: Hysteresis Loops for SDOF System with P-TMFD and SA-TMFD
(a) P-TMFD; (b) SA-TMFD ($\alpha=0.9999$); (c) SA-TMFD ($\alpha=0.999$);
(d) SA-TMFD ($\alpha=0.99$); (e) SA-TMFD ($\alpha=0.98$); (f) SA-TMFD ($\alpha=0.97$);
(g) SA-TMFD ($\alpha=0.96$); (h) SA-TMFD ($\alpha=0.95$); (i) SA-TMFD ($\alpha=0.90$)



plotted against the SA-TMFD stroke. Figure 2(a) shows the hysteretic loop for the P-TMFD in its stick-slip states. In this figure vertical line shows the stick state of the damper, while the slip state is spotted by horizontal lines. It is observed from the Figure 2(b) to 2(i), that SA-TMFD headed to elliptical hysteretic loops. The absence of vertical lines in hysteretic loop shows that the damper remains in slip state all the time during the harmonic excitation. It is also observed that as the value of α decreases the loop becomes flat ellipse while when the value of α increases and reaches close to one, it is possible that the SA-TMFD may enter in stick state for certain time instants as shown in Figure 2(b), which may affect the energy dissipation capacity of the SA-TMFD. Thus, the performance of SA-TMFD depends on the value of α as it controls the geometric shape of hysteretic loops. Also, by selecting an appropriate value of α , one can keep SA-TMFD continuously in slip mode and utilize its energy dissipation capacity effectively.

Numerical Study for Earthquake Excitation

In this section, the response of primary system with SA-TMFD subjected to earthquake ground acceleration is investigated. The

earthquake time histories along with their Peak Ground Acceleration (PGA) and components which are used for this study are represented in Table 1. The displacement and acceleration response spectra of the above mentioned earthquakes are shown in Figure 3 for 2% critical damping. The maximum ordinate of acceleration are 1.225 g, 3.616 g, 3.296 g, 3.614 g, occurring at the period of 0.46 s, 0.64 s, 0.08 s and 0.36 s for Imperial Valley, Loma Prieta, Landers and Kobe earthquakes, respectively. The spectra of these ground motion indicate that these ground motions are recorded on a rocky site or on a firm soil.

The controlling parameter α on which the efficiency of SA-TMFD depends is discussed here. The response quantities of the interest considered for the study are peak values of structural displacement, structural acceleration and damper displacement.

Effect of Controlling Parameters on the Performance of P-TMFD and SA-TMFD

The effect of controlling parameter R_f (i.e., maximum friction force of the damper normalized by the weight of the P-TMFD), on the performance of the P-TMFD is shown in

Table 1: Details of Earthquakes Considered for Numerical Study

Earthquake	Recording Station	Component	Duration (s)	PGA (g)
Imperial Valley (19 th May 1940)	El Centro Array # 9	I – ELC 180	40	0.313
Loma Prieta (18 th October 1989)	UCSC 16 LOS Gatos Presentation Centre (LGPC)	LGP 000	25	0.96
Landers 28 th June 1992	Lucerene Valley	LCN 275	48.125	0.721
Kobe 16 th January 1995	Japan Meteorological Agency (JMA) 99999 KJMA	KJM 000	48	0.82

Figure 3: Displacement and Acceleration Spectra of Four Earthquakes Considered for the Study

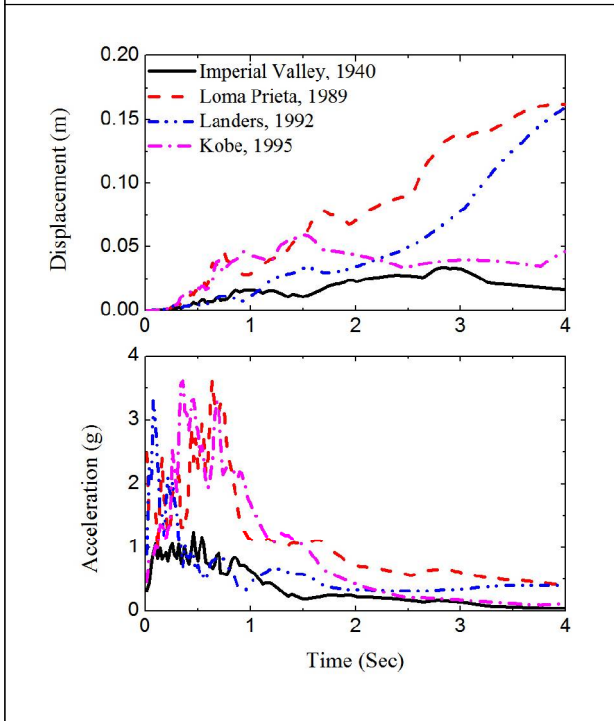


Figure 4: Effect of R_f on Performance of P-TMFD

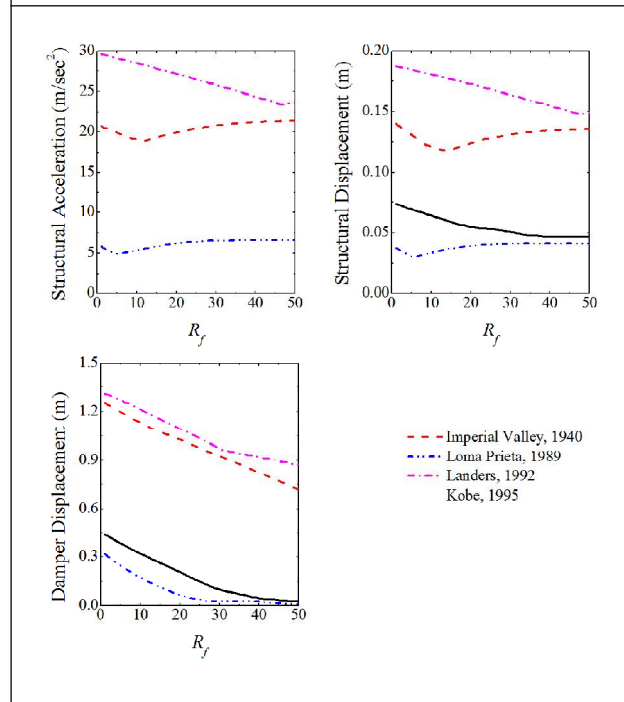
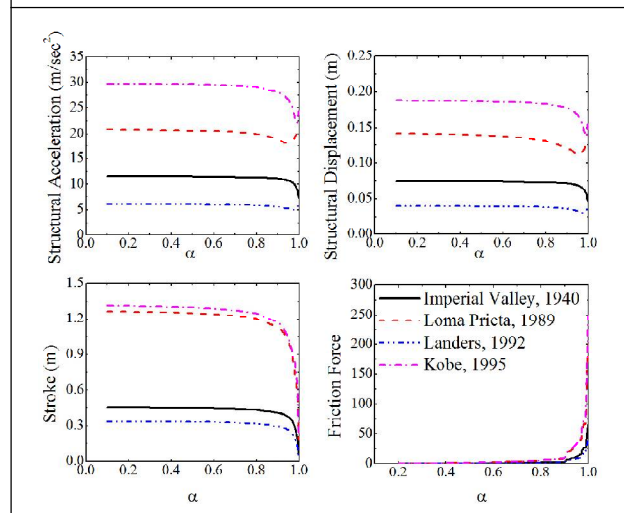


Figure 4. In this figure the structural displacement, structural acceleration and damper displacement developed in the damper are plotted against the R_f . It is observed that as the value of R_f increases the response of the system decreases and further increases with the increase in the value of R_f . It shows that each earthquake has an optimum value of R_f for which the response of the system attains minimum value. The optimum value of R_f is 40%, 14%, 5% and 48%, for Imperial Valley, Loma Prieta, Landers and Kobe earthquakes, respectively. The variation of the optimum value of R_f for different earthquake is due to their different dynamic characteristic.

Similarly, the effect of controlling parameter α on the performance of the SA-TMFD is

Figure 5: Effect of α on performance of SA-TMFD



shown in the Figure 5. In this figure, structural displacement, structural acceleration, damper displacement and friction force developed in the damper are plotted against α . It is observed that as the value of α increases the structural displacement, acceleration and

stroke decreases and frictional force in the damper increases. It is also observed that for a given earthquake excitation an optimum value of α exists at which the response of the system attains minimum value. The variation of the optimum value of α for different earthquake is due to their different dynamic characteristic. The optimum value of α is about 0.999, 0.95, 0.977 and 0.99, for Imperial Valley, Loma Prieta, Landers and Kobe earthquakes, respectively.

Effect of PGA on Response

In order to study the effect of PGA on the responses of interest, the PGA of earthquake time histories are scaled from 0.05 g to 1.0 g. The peak displacement, peak acceleration and peak damper displacement of a SDOF system with P-TMFD, SA-TMFD and uncontrolled system are plotted against the different PGA level for various earthquakes in Figures 6, 7 and 8. For comparison, the

Figure 7: Peak Acceleration Responses of P-TMFD and SA-TMFD Under Different Earthquakes: (a) Imperial Valley, 1940; (b) Loma Prieta, 1989; (c) Landers, 1992; (d) Kobe, 1995

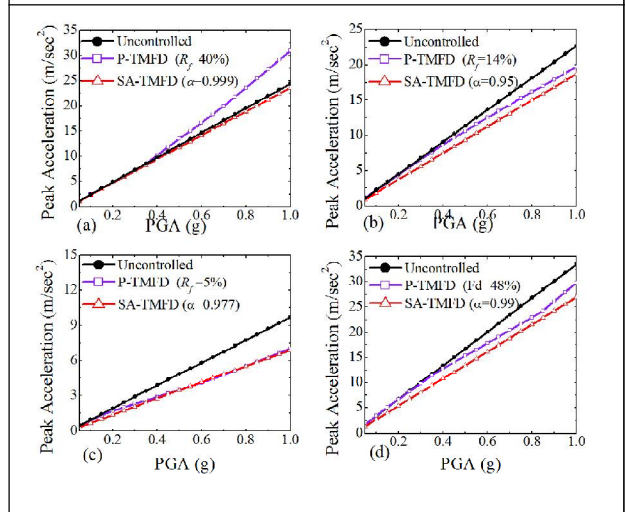


Figure 8: Peak Damper Displacement Responses of P-TMFD and SA-TMFD Under Different Earthquakes: (a) Imperial Valley, 1940; (b) Loma Prieta, 1989; (c) Landers, 1992; (d) Kobe, 1995

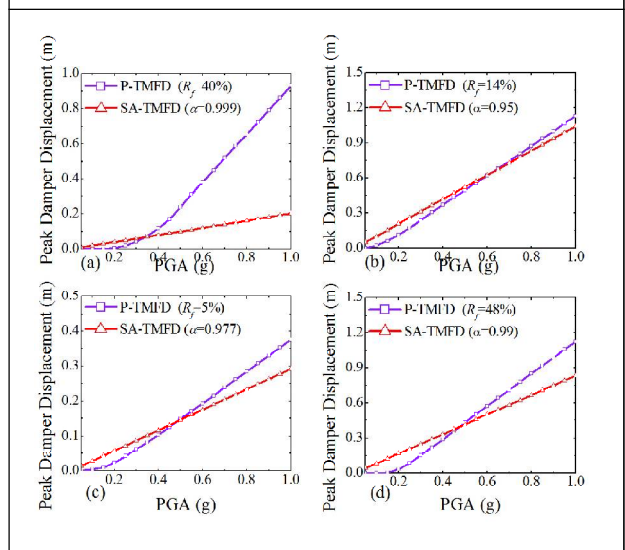
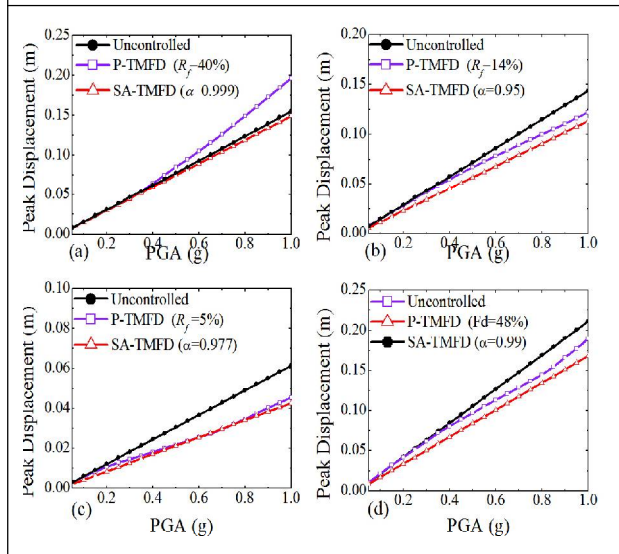


Figure 6: Peak Displacement Responses of P-TMFD and SA-TMFD Under Different Earthquakes: (a) Imperial Valley, 1940; (b) Loma Prieta, 1989; (c) Landers, 1992; (d) Kobe, 1995



responses of P-TMFD are plotted for the optimum value of R_f of each earthquake as obtained in earlier section. Also, the responses of SA-TMFD are plotted for optimum values of α . It is observed that for Imperial Valley

earthquake the response of the P-TMFD is greater than that of uncontrolled system, which shows that it is amplifying the response of SDOF system, may be due to the off-tuning of the P-TMFD. For other earthquakes P-TMFD is reducing the response of the SDOF system effectively for larger PGA levels while in case of lower PGA levels it is performing close to the uncontrolled system. The reason behind this is that for lower PGA levels the P-TMFD may not be activated or underperforming. It is also observed that the SA-TMFD can be activated at all PGA levels and is also effective in reducing the response of the SDOF system at all PGA levels, due to this SA-TMFD overcomes all the limitations of P-TMFD.

In a similar manner, Figures 9, 10, 11 and 12 depicts the displacement and acceleration

Figure 9: Comparison of Acceleration and Displacement Responses of Uncontrolled, P-TMFD and SA-TMFD for Imperial Valley Earthquake (1940) for PGA as 0.4 g and 0.9 g

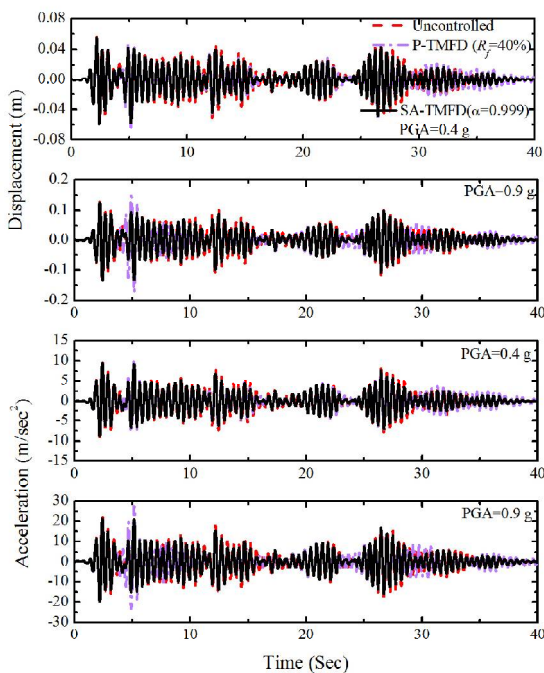


Figure 10: Comparison of Acceleration and Displacement Responses of Uncontrolled, P-TMFD and SA-TMFD for Loma Prieta Earthquake (1989) for PGA as 0.4 g and 0.9 g

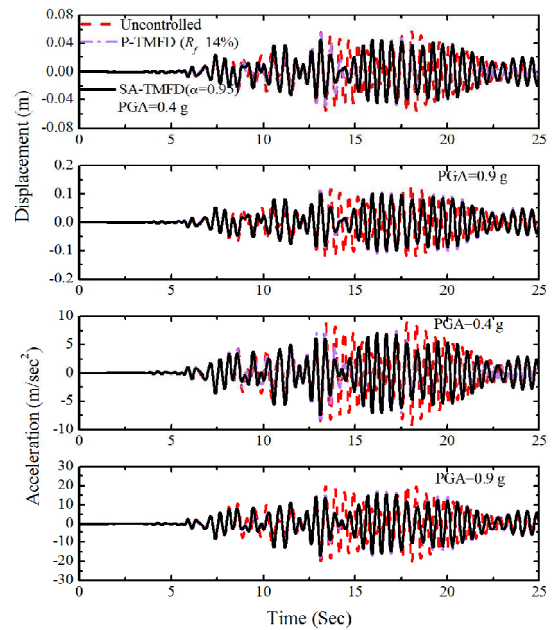


Figure 11: Comparison of Acceleration and Displacement Responses of Uncontrolled, P-TMFD and SA-TMFD for Landers Earthquake (1992) for PGA as 0.4 g and 0.9 g

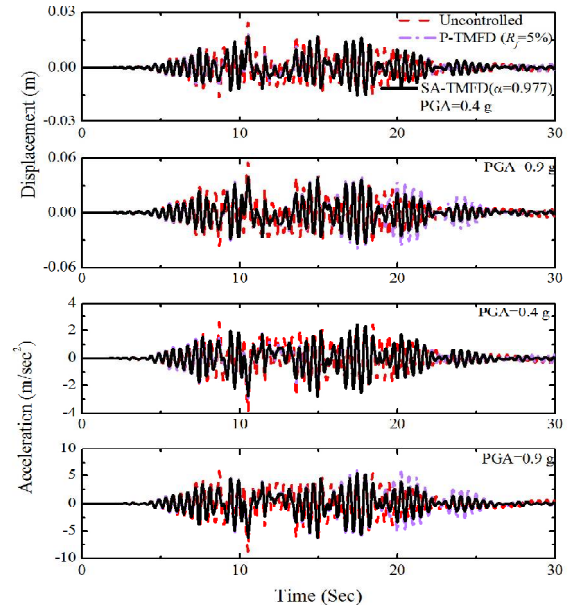
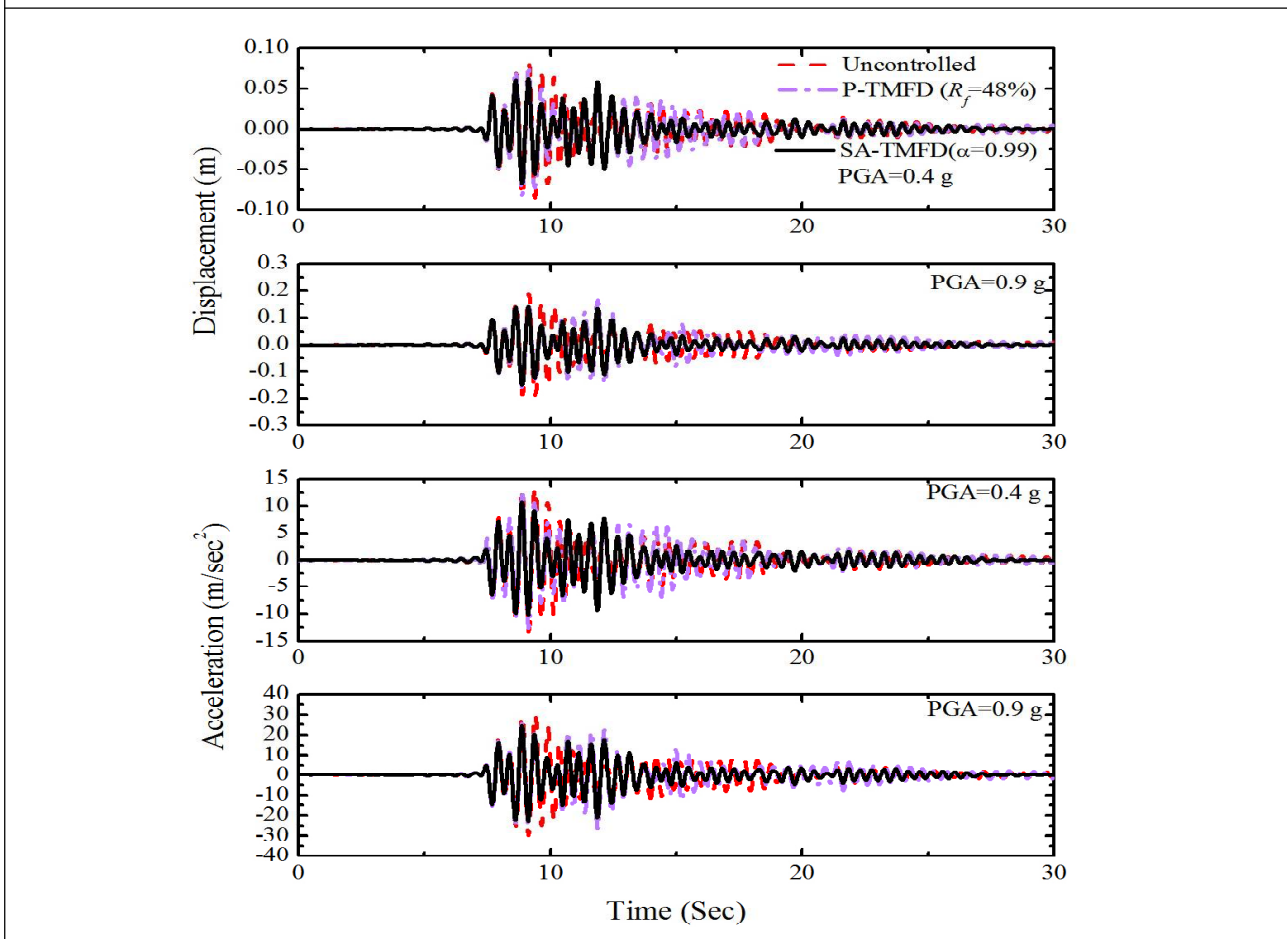


Figure 12: Comparison of Acceleration and Displacement Responses of Uncontrolled, P-TMFD and SA-TMFD for Kobe Earthquake (1994) for PGA as 0.4 g and 0.9 g



time history of a SDOF system with P-TMFD, SA-TMFD and uncontrolled system for optimum value of R_f and α . For this purpose, the PGA of all the considered earthquakes are scaled to 0.4 g and 0.9 g, which shows the low and high intensity level earthquakes, respectively. The time history responses of the system confirms that the SA-TMFD are more effective than P-TMFD in response reduction of the SDOF system as it is activated at such a lower and higher PGA levels.

Effect of Variation of Mass Ratio and Tuning Ratio

Figures 13 and 14 depict the effectiveness of

control algorithm, when assuming the changes in the parameters or properties of the P-TMFD and SA-TMFD. For this purpose, the response of P-TMFD and SA-TMFD is plotted against the varying mass ratio and tuning ratio in Figures 13 and 14, respectively. It is observed that the response of the system is relatively less sensitive to the change in mass ratio of the system. While, in case of change in the tuning property of the system, it is more sensitive. It is also observed that the responses of interest are more sensitive for the SA-TMFD in compare to responses of P-TMFD. So, even if the actual friction force applied at SA-TMFD is different (due to change in properties/

Figure 13: Effect of Percentage Variation in the Mass Ratio of SA-TMFD (a) P-TMFD and (b) SA-TMFD

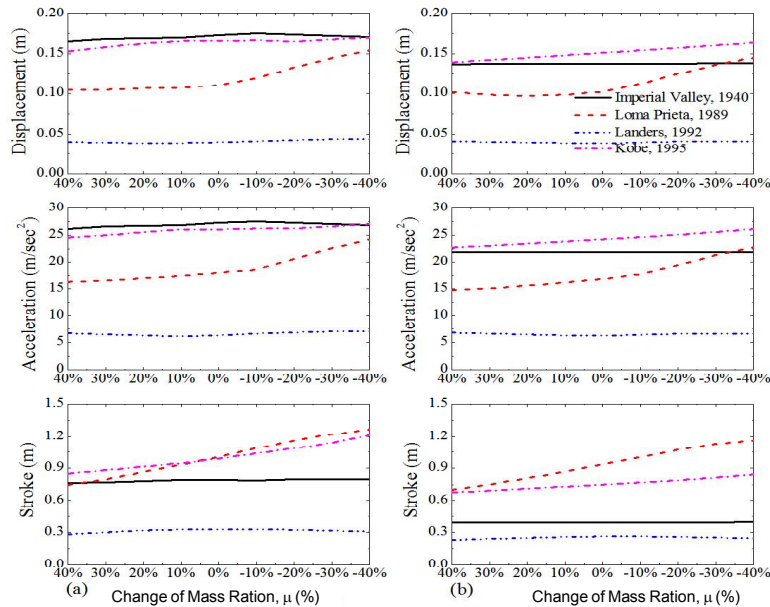
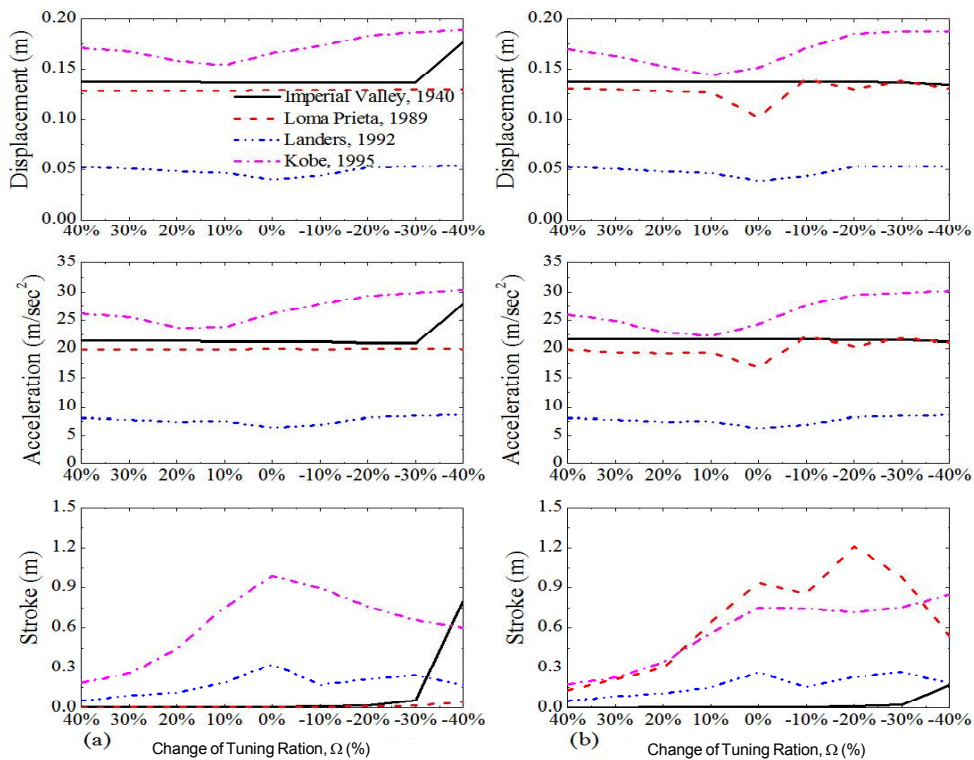


Figure 14: Effect of Percentage Variation in the Tuning Ratio of SA-TMFD (a) P-TMFD and (b) SA-TMFD



parameters of SA-TMFD) than that of the friction force calculated from Predictive control law, SA-TMFD slightly alters the responses of the system.

CONCLUSION

The response of a SDOF system attached with a P-TMFD and SA-TMFD is investigated for harmonic and earthquake excitations. The Predictive control law proposed by Lu (2004) is used for this study as it produces continuous and smooth slip force throughout the duration of an excitation. The differential equations of motion are solved numerically using state-space method. To investigate the effectiveness of SA-TMFD with predictive control, the response of the structure with P-TMFD are compared with the responses of the structures with SA-TMFD. From the trends of results of the present study, the following conclusions may be drawn.

1. The performance of SA-TMFD depends on the value of α as it controls the geometric shape of hysteretic loops.
2. By selecting an appropriate value of α one can keep SA-TMFD continuously in slip mode and utilize its energy dissipation capacity effectively.
3. For a given earthquake excitation an optimum value of α exists at which the response of the system attains minimum value. The variation of the optimum value of α for different earthquake is due to their different dynamic characteristic.
4. SA-TMFD can be activated at all PGA levels and is also effective in reducing the response of the SDOF system at all PGA levels, due to this SA-TMFD overcomes all the limitations of P-TMFD.

5. If the actual friction force applied at SA-TMFD is different (due to change in properties/ parameters like mass ratio and tuning ratio of SA-TMFD) than that of the friction force calculated from Predictive control law, SA-TMFD slightly alters the responses of the system.

REFERENCES

1. Akbay Z and Aktan H M (1995), "Abating earthquake effects on buildings by active slip brace devices", *Shock and Vibration*, Vol. 2, No. 2, pp. 133-142.
2. Bhaskararao A V and Jangid R S (2006), "Seismic analysis of structures connected with friction dampers", *Engineering Structures*, Vol. 28, pp. 690-703.
3. Constantinou M, Mokha A and AM, R (1990), "Teflon bearing in base isolation, Part II: modeling", *Journal of Structural Engineering (ASCE)*, Vol. 116, pp. 455-474.
4. Dowdell D J and Cherry S (1994), "Structural control using semi-active friction dampers", *Proceedings of the First World Conference on Structural Control*, Los Angeles, Vol. 3; FAI-pp. 59-68.
5. Dowdell D J and Cherry S (1996), "On passive and semi-active friction damping for seismic response control of structures", *Proceedings of the 11th World Conference on Earthquake Engineering*, Acapulco, Mexico, Paper 957.
6. Gewei Z and Basu B (2010), "A Study on friction-tuned mass damper: Harmonic

- solution and statistical linearization”, *Journal of Vibration and Control*, Vol. 17, pp. 721-731.
7. Inaudi J A (1997), “Modulated homogeneous friction: A semi-active damping strategy”, *Earthquake Engineering and Structural Dynamics*, Vol. 26, No. 3, pp. 361-376.
 8. Kannan S, Uras H M and Aktan H M (1995), “Active control of building seismic response by energy dissipation”, *Earthquake Engineering and Structural Dynamics*, Vol. 24, No. 5, pp. 747-759.
 9. Lin C C, Ling G L and Wang J F (2010), “Protection of seismic structures using semiactive friction TMD”, *Earthquake Engineering and Structural Dynamics*, Vol. 39, pp. 635-659.
 10. Lu L Y and Lin G L (2002), “Seismic protection of structures using semi-active friction dampers”, *Proceedings of the 9th international conference on computing in Civil and Building Engineering*, Taipei, 3-5 April, 2002; pp. 537-542.
 11. Lu L Y (2004), “Predictive control of seismic structures with semi-active friction dampers”, *Earthquake Engineering and Structural Dynamics*, Vol. 33, No. 5, pp. 647-668.
 12. Meirovitch L (1990), *Dynamics and control of structures*, John Wiley & Sons, Inc., New York.
 13. Ricciardelli F and Vickery B J (1999), “Tuned vibration absorbers with dry friction damping”, *Earthquake Engineering and Structural Dynamics*, Vol. 28, pp. 707-723.
 14. Spencer Jr B F, Dyke S J, Sain M K and Carlson J D (1997), “Phenomenological model for magnetorheological dampers”, *Journal of Engineering Mechanics (ASCE)*, Vol. 123, No. 3, pp. 230-238.
 15. Wen Y K (1976), “Method for random vibration of hysteretic systems”, *Journal of Engineering Mechanics (ASCE)*, Vol. 102, pp. 249-263.
-